

---

# CRONOS: Benchmarking Counterfactual Physical Consistency in Video Models

---

**León Begiristain**

University of Freiburg  
Freiburg im Breisgau, Germany  
begirist@cs.uni-freiburg.de

**Olaf Dünkel**

Max Planck Institute for Informatics  
Saarland Informatics Campus, Germany  
oduenkel@mpi-inf.mpg.de

**Adam Kortylewski**

CISPA Helmholtz Center for Information Security  
Saarbrücken, Germany  
kortylewski@cispa.de

## Abstract

Video prediction is increasingly viewed as a path toward generalizable world models, yet it remains unclear whether these systems learn underlying causal structure or merely exploit superficial visual correlations for future prediction. We introduce CRONOS, an intervention-based benchmark designed to evaluate counterfactual physical consistency: whether a model’s predictions of physical events respond appropriately to controlled changes in the visual input, such as variations of scene context, viewpoint, object appearance, and object category. Built in a photorealistic Unreal Engine environment, CRONOS enables controlled, high-fidelity generation of videos across diverse scenes and dynamics. In contrast to previous benchmarks, CRONOS systematically intervenes on four key factors — viewpoint, scene, object category, and object appearance — while keeping the underlying physical event type, such as a collision, occlusion, or fall, fixed. Our evaluation of recent open-source video generators reveals substantial failures in counterfactual physical consistency: prediction quality for the same physical event type is affected by appearance, environment, and, particularly by viewpoint changes. CRONOS provides a controlled and reproducible testbed for diagnosing how the quality of generated videos changes for different interventions, establishing a concrete target for developing models that perform consistently across changes of multiple conditions. The dataset and code are available at: <https://genintel.github.io/CRONOS/>.

## 1 Introduction

Recent progress in generative video modeling has made it increasingly plausible to learn *world models*—predictive models that capture how the visual world evolves over time and can support downstream reasoning and planning [19]. Large-scale video diffusion models can synthesize temporally coherent, high-fidelity futures from partial observations, fueling the belief that scaling video prediction may yield generalizable predictive models of real-world dynamics [22, 21]. However, visual realism alone does not imply that these predictive systems develop *causal representations* [42] that capture relationships between objects, scenes, and dynamics, allowing robust predictions to remain stable under changes in viewpoint, appearance, or context. Such structured, causally meaningful representations are widely believed to be essential for robust generalization, compositional reasoning, and decision-making, as they enable models to distinguish underlying world dynamics from incidental

## Are video models physically consistent under visual interventions?

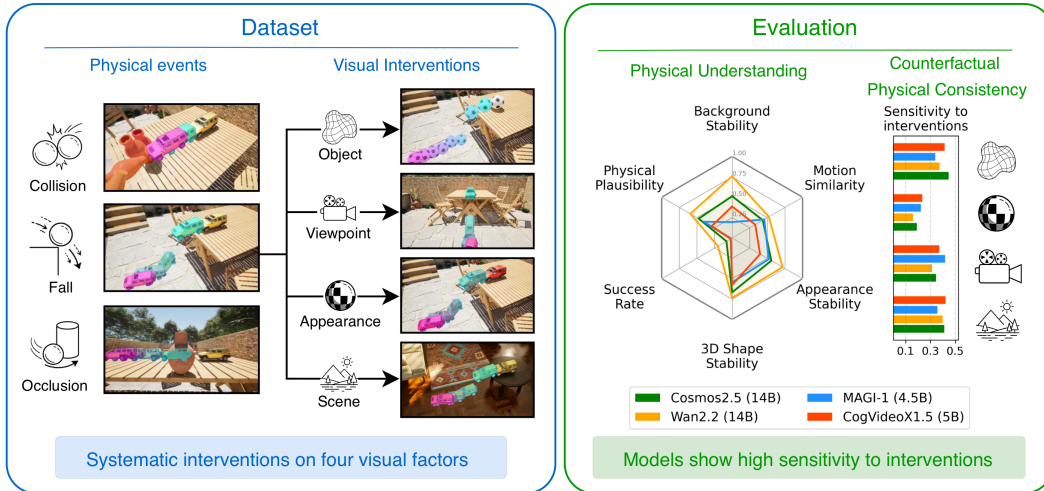


Figure 1: **The CRONOS Benchmark.** A benchmark for evaluating counterfactual physical consistency: whether a model’s predictions of physical events respond appropriately to controlled changes in the visual input.

visual correlations [38, 41]. Despite rapid progress in video generation, it remains unclear whether modern models acquire such representations or primarily rely on superficial statistical regularities in the data for prediction. Studying this gap requires principled evaluations that move beyond perceptual quality and directly test whether a model’s predicted future responds appropriately to controlled changes in the visual input.

Existing work has begun to probe whether video models capture physical and causal structure through specialized evaluation benchmarks. Some approaches construct controlled physics scenarios and assess predictions by comparing generated outcomes against ground-truth trajectories or physical constraints, measuring whether models obey expected dynamics such as collisions, motion, or conservation laws [36, 52]. Other methods rely on object-centric analyses, evaluating predicted trajectories or interactions using tracking and segmentation pipelines [48, 30], or employ vision–language models and human judgments to detect violations of physical plausibility [2]. While these benchmarks provide valuable insights into physical correctness and perceptual realism, they largely evaluate predictions under a *fixed visual observation*. As a result, they reveal whether a model can produce a plausible continuation of a given scene, but provide limited insight into whether the underlying predictive representation is stable and structured. A reliable model should remain stable under nuisance changes such as viewpoint or appearance variations, while adapting coherently when other aspects of the scene change. We formalize this requirement through the notion of *counterfactual physical consistency*:

**Counterfactual physical consistency** refers to a model’s ability to produce predictions of physical events that remain coherent across counterfactual variants of the visual input.

To study counterfactual physical consistency in modern video models, we introduce **CRONOS**, an intervention-based benchmark designed to evaluate how predictive video models respond to controlled changes in the visual world. CRONOS is built in a photorealistic Unreal Engine environment to enable the generation of realistic video sequences in which the underlying physical event type remains fixed while specific visual factors are systematically varied. In particular, we intervene along four complementary dimensions: camera viewpoint, scene, object category, and object appearance. Viewpoint and appearance changes primarily test robustness to nuisance variations that preserve physical parameters, while object-category and scene interventions probe whether models adapt coherently across changes in object properties and layouts. The benchmark spans across three canonical interaction scenarios—including collisions, rolling and falling, and occlusion and reappearance—chosen to isolate fundamental forms of basic physical interaction. By explicitly controlling and recombining these factors, CRONOS enables fine-grained analysis of counterfactual

physical consistency in video models. Finally, the full factorial evaluation consists of 3 events, 5 scenes, 5 object categories, up to 4 viewpoints, and 3 appearances, resulting in a total of 675 videos; viewpoint variation is omitted for occlusion to preserve the visibility structure.

For evaluation, we introduce object-centric metrics that disentangle 3D motion from appearance, enabling a more fine-grained assessment of generation fidelity. Additionally, our intervention framework measures each model’s sensitivity to controlled changes in the input signal, which serves as diagnostics of counterfactual consistency. We apply these metrics to several state-of-the-art open-source video generation models under both image-to-video (I2V) and video-to-video (V2V) settings.

Our analyses reveal that models often fail to generate physically consistent videos and show substantial variation across intervention types, with especially high sensitivity for viewpoint and object type changes. Further, we show that video conditioning improves over image conditioning, and that scaling model size does not necessarily lead to more consistent generation quality. We provide the videos and metadata of the benchmark, as well as code for reproducing the evaluation metrics. An overview of the data generation and evaluation in CRONOS can be found in Figure 1.

## 2 Related Work

**Video generation models.** Recent advances in video generation have produced models capable of synthesizing temporally coherent and visually detailed videos that are conditioned on text (T2V), images (I2V), past video frames (V2V), or combinations thereof. Early work extended image diffusion models to the temporal domain by inserting temporal layers into latent diffusion architectures [9, 44, 8, 21]. More recently, transformer-based diffusion architectures (DiTs) [33] have enabled models such as CogVideoX [50], Wan [49], HunyuanVideo [29], and MovieGen [39] to generate high-fidelity video at scale. Further, autoregressive formulations allow arbitrarily long generated sequences, as demonstrated by MAGI-1 [45] and COSMOS [1]. However, despite advances in terms of visual fidelity, recent studies have shown that these models frequently violate basic physical principles such as object permanence, gravity, and cause-effect relations [36, 27]. This suggests that such models are limited in their ability to generalize physical understanding beyond visual patterns seen during training. While recent efforts [30] explored physics-aware post-training to mitigate such failures, these approaches still do not guarantee robustness. These findings highlight a crucial gap in current video generation models that CRONOS aims to evaluate systematically: counterfactual physical consistency, the capability of generating videos of physical events in consistent quality even when scene parameters change.

**Evaluating video generation.** Early evaluations of video generation models focused on image-based metrics to evaluate generation quality, such as FVD [47], and were extended to capture various quality metrics [25, 24, 32, 15]. A growing set of benchmarks targets physical realism more directly where physical commonsense, physical laws, or scientific concepts are evaluated by human, VLMs, or learned evaluators [5, 6, 35, 12, 17, 18, 23, 31, 54, 16]. Reference-based evaluations compare generations to trajectories, physical equations, real or simulated experiments [30, 36, 52, 48, 53]. Specifically, PISA [30] compares object trajectories of videos that cover objects in free fall scenarios. Physics-IQ [36] evaluates videos in real-world physical experiments through image-based metrics. In contrast, Morpheus [52] measures physics-informed scores of generated videos, specifically evaluating whether equations of motion are satisfied. WorldBench [48] estimates physical parameters of generated videos based on simple real-world physical experiments and compares results to synthetic videos that were acquired from a simulation environment. These works expose important failures, but they generally evaluate independent prompts or individual reference events rather than changes under controlled interventions, a perspective motivated by robustness evaluations [20, 43, 13]. In contrast, CRONOS enables a comprehensive study of how generated videos vary under controlled interventions by employing a high-fidelity physical simulator that renders reference videos at high visual fidelity, allowing for an analysis of counterfactual generation that has not directly been addressed by prior video-generation benchmarks.

**Simulators for probing visual understanding.** Synthetic environments enable controlled tests that are difficult to obtain from real videos. Many benchmarks make use of synthetic data in the realm of video reasoning: CRAFT [3], CLEVRER [51] and GRASP [26], design pairs of questions and videos and evaluate models’ understanding on simple scenes, while IntPhys [10] focuses on



Figure 2: **CRONOS dataset overview.** Examples illustrating the three physical events (rows) used in the CRONOS benchmark: collision, fall, and occlusion. For each event instance, we render multiple counterfactual observations by varying factors such as scene context, camera viewpoint, object category, and object appearance. Colored overlays show object trajectories across time, visualizing the underlying motion dynamics. This controlled design enables systematic evaluation of whether video models produce consistent predictions across different observations of the same event setup.

detection of violations of physics. From the modeling perspective, Physion [7, 46] evaluated different architecture’s ability to predict the outcome of diverse physical events and PhysWorld [27] designed simple 2D environments to study generalization of visual properties on video diffusion. More recently, PISA [30] employed synthetic data to fine-tune and enhance physics modeling abilities on video models, while WorldBench [48] generated synthetic scenes to evaluate physical understanding. Yet, most benchmarks leveraging synthetic data rely on basic objects with flat or simple textures, and do not make use of high-fidelity rendering tools able to realistically simulate lights and shadows. In contrast, CRONOS relies on a photorealistic simulator, keeping the advantages of a controlled environment while using higher-fidelity visual content than many synthetic physics benchmarks.

### 3 CRONOS Benchmark

CRONOS frames the evaluation of video generation models as a controlled counterfactual experiment. The core experimental unit in CRONOS is a *physical event*: a basic physical simulation specified via initial states, impulses, and simulator parameters that defines the underlying 3D dynamics of a scene. From each event type, we render a set of *counterfactual observations* by intervening on a single factor at a time—camera viewpoint, scene, object appearance, or object category—while holding the remaining variables fixed. Some interventions preserve the underlying physical parameters, such as viewpoint and appearance, while others change contextual or object-level properties that may alter the expected rollout. This design enables measurement of *counterfactual physical consistency*: whether model predictions remain stable under nuisance interventions that do not alter the event dynamics (e.g., viewpoint) and vary coherently when interventions induce structured changes (e.g., object class). The remainder of this section describes our controlled simulation pipeline for generating event instances (Section 3.1), the set of canonical physical events defining underlying dynamics (Section 3.2), the systematic intervention protocol used to render counterfactual observations (Section 3.3), and the object-centric metrics used to quantify prediction accuracy and intervention sensitivity (Section 3.4).

#### 3.1 Data Generation

We generate all sequences in a controllable Unreal Engine environment [14]. Each event is specified by carefully selected simulator configurations, allowing targeted interventions of individual factors of realistic events. This control is difficult to obtain from real video, where camera viewpoint, object appearance, scene context, and dynamics cannot be independently varied while preserving the same physical event type. All scenes are rendered at  $1920 \times 1080$  pixels and 30 FPS using high-quality professional 3D assets chosen to reflect common real-world environments, including indoor and outdoor environments under diverse lighting conditions. In addition to RGB frames, the simulator provides per-object segmentation masks, used for the object-centric metrics in Section 3.4. We show

examples of rendered scenes for all physical events in Figure 2. A detailed description of the dataset statistics can be found in Section A.

### 3.2 Physical Events

CRONOS uses three physical events that probe complementary aspects of predictive reasoning while keeping the setup compact. All are generated from standardized initial conditions in which an impulse initiates object motion. So, differences across intervention variants come from the controlled visual change rather than a new event setup. We consider three scenarios:

**Fall (roll-to-drop).** A single object rolls across a surface and falls from an edge, testing prediction across changing contact conditions and free-fall motion.

**Collision.** One object impacts another, testing whether generated videos preserve physically plausible interaction dynamics, including temporal and spatial coherence and object permanence.

**Occlusion.** An object rolling across a smooth surface becomes fully occluded behind another scene element and later reappears, which tests the capability to capture long-range temporal coherence and infer hidden motion.

Together, these events provide controlled yet diverse dynamic settings that are employed for the systematic analysis of counterfactual consistency via interventions as introduced in the following.

### 3.3 Systematic Visual Interventions

Building on the controlled simulation setup (Section 3.1) and physical event dynamics (Section 3.2), CRONOS systematically renders a set of interventions. For sensitivity analysis, we group variants that differ along one intervention axis while holding the remaining variables fixed:

**Scene intervention.** The background environment and scene layout details are changed (e.g., height in fall sequences), which tests whether models remain reliable across contextual changes and adapt to layout-dependent dynamics when scene geometry affects the rollout.

**Camera viewpoint intervention.** The rendering viewpoint is changed while keeping scene dynamics intact, probing whether models can disentangle scene geometry from observed motion while maintaining perspective consistency.

**Object appearance intervention.** Visual object attributes, such as color, are changed without altering physical parameters, isolating whether models correctly disentangle appearance from dynamics.

**Object-category intervention.** The object of interest is replaced with another compatible object, changing both visual properties (e.g., shape, material) and physical parameters (e.g., mass, friction), which directly affect motion dynamics. This intervention probes whether models adjust predictions coherently across object instances whose visual and physical properties differ, or instead rely on object-specific correlations learned during training.

The dataset follows a full-factorial design for each physical event, except viewpoint, which is fixed for occlusion events in order to preserve the intended visibility structure. This enables fine-grained analysis of sensitivities and counterfactual consistency in generated videos.

### 3.4 Evaluation Metrics

CRONOS decomposes generation quality into complementary per-video metrics: appearance stability, background stability, 3D-shape stability, motion similarity, and physical plausibility, and a global success criterion that aggregates them into a single pass/fail signal per video. All reported quality scores are normalized to  $[0, 1]$  and higher values always indicate superior performance. Detailed descriptions of all metrics and additional steps such as segmentation masks, visibility filtering, aggregation rules, and thresholds are described in Section C.

**Appearance stability** measures whether each object preserves its visual identity over time, using cosine similarities of per-object DINOv2 [37] embeddings compared to the initial frame, as in VBench [25]. CLS tokens are computed from images with the background masked out.

**Background stability** measures whether the background regions remain coherent and fixed relative to the conditioning frame by computing pixel-wise error, following WorldBench [48]. It captures artifacts such as background morphing, lighting drift, camera motion, and new objects, all of which are undesired and explicitly mentioned in the text prompt (Table 4).

**3D-shape stability** measures whether object geometry remains stable by computing per-object meshes reconstructed by SAM3D [11] across time and comparing them to the initial frame mesh via the Chamfer distance.

**Motion similarity** measures agreement between generated and reference motion via the cosine similarity of the embeddings computed by the appearance-invariant motion encoder from DisMo [40].

**Physical plausibility** measures high-level event correctness and physical violations using a VLM-as-judge protocol [34, 54] with Qwen3-VL-32B [4]. This fixed set of video-specific binary questions cover common physical violations and event-completion criteria.

**Success rate** aggregates per-video metrics into a binary pass/fail criterion. A video is counted as successful only if all quality metrics pass their calibrated thresholds and no object disappearance is detected. Thresholds are calibrated from the human study in Section 4.2 by requiring equal ratios of false positive and false negative rates, where failed videos received low annotator quality rating for the corresponding metric. Further, the disappearance detector prevents segmentation failures from producing artificially high object-centric scores. The success rate is the fraction of videos that pass this test.

**Sensitivity to interventions.** Beyond per-video physical evaluation, we measure how much each intervention changes the quality of the generated output along the presented metrics. For this, we compute the deviation between the best and the worst performance for a set of experiments that differ only along one intervention axis and average across groups and metrics. A lower sensitivity is generally better, as it indicates higher **counterfactual consistency**: the model’s output quality remains stable across controlled interventions. Sensitivity serves as a complementary diagnosis axis to the absolute metrics.

## 4 Results

In the following, we present the model evaluations using our developed framework and discuss our findings. After clarifying the experimental setup in Section 4.1, we present the user study used to validate the selected metrics in Section 4.2 before discussing the benchmark’s findings in Section 4.3.

### 4.1 Experimental Setup

Our evaluation includes several state-of-the-art open-source video generation models: Cosmos2.5 [1], CogVideoX1.5 [50], MAGI-1 [45], and Wan2.2 [49]. For Cosmos, we evaluate the two available model sizes 2B and 14B to study the effect of model scaling in video generation models. All models are evaluated in the I2V setting using the first frame. In addition, we also evaluate Cosmos and MAGI-1 in the V2V setting using five conditioning frames, which reveal initial direction and velocity while still requiring future prediction capabilities.

We use each model’s standard settings and the same event-specific prompt template that describes the scene configuration, contextual details, and intended motion. Detailed text prompts can be found in Section B and qualitative examples of generated videos are shown in Figure 3.

As input signals do not determine all underlying scene parameters, multiple plausible futures exist, particularly in the I2V case. To account for this effect, we sample three seeds per experiment and report a best-of-three score by selecting the seed with the most similar motion to the reference video. When computing sensitivities, we select the seed with the best motion score averaged across the intervention variants.

### 4.2 Human Evaluation Study

To validate our selected metrics, we perform a user study that ranks generated videos along the evaluated dimensions. Specifically, we hire qualified annotators via Prolific and ask them to label the quality of *object appearance*, *object shape*, *background stability*, *motion plausibility*, and *event*

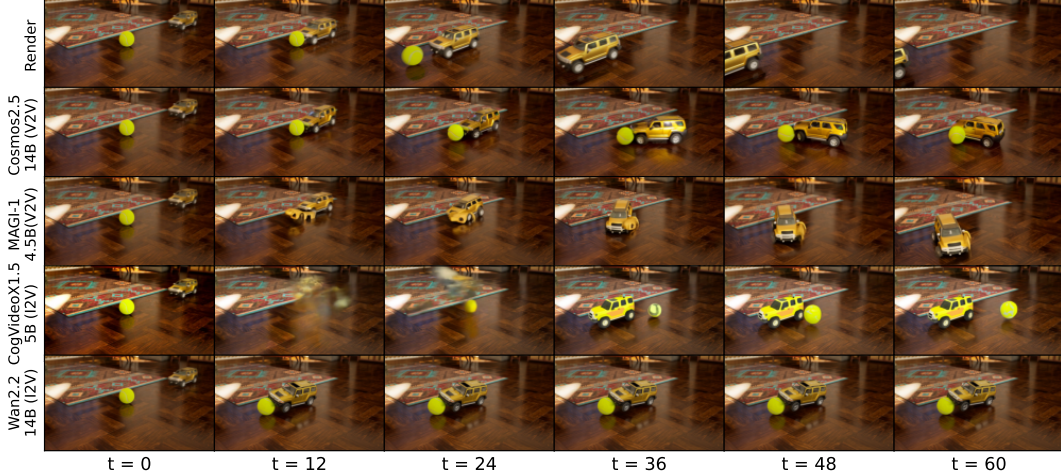


Figure 3: **Qualitative comparison of multiple video generation models on CRONOS.** Generated futures for a collision event are compared with the ground-truth render for successive frames. While most models preserve coarse scene structure, they fail to maintain consistent object dynamics, exhibiting trajectory drift, incorrect physical interactions, or object identity distortions over time.

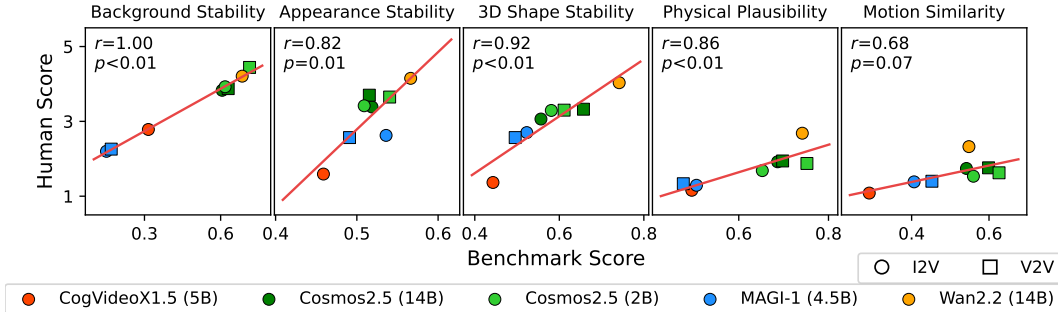


Figure 4: **Results of the human evaluation study.** Model performances positively correlate with human ratings (higher is better), as the Pearson correlation coefficients indicate.

*quality.* We follow [6] and evaluate on a scale between 1 (very poor) and 5 (excellent). We select 540 representative videos from various models with diverse objects and scenes, and we collect median-aggregated ratings of three annotators. More details including annotation instructions are provided in Section D. We provide Pearson correlation coefficients for measured performance vs. human rating in Figure 4. The positive correlations support using the proposed metrics for the subsequent analysis on the complete benchmark.

### 4.3 Analysis of Benchmarking Results for Video Models

Having introduced the CRONOS benchmark, we now discuss the findings following our benchmark analysis. Extended results can be found in Section H.

**Physical event generation.** As CRONOS covers fundamental rigid-body interactions, the averaged metrics in Table 1 provide diagnostic evidence about each model’s ability to generate videos of physically valid events. All models achieve comparably low scores across the evaluated metrics but model performance substantially differs, with Cosmos models and Wan2.2 performing the best and MAGI-1 and CogVideoX1.5 being clearly worse across the evaluated metrics. Because a video is counted as successful only when all metrics pass their calibrated thresholds, overall success rates are low: Cosmos2.5-2B (V2V) and Wan2.2 (I2V) achieve 0.22 and 0.20 respectively, while the remaining models range from 0.01 to 0.14. All models mostly fail on at least one quality dimension, consistent with our human evaluation study. We provide the numerical results of the human study and per-metric success rates in the supplementary Section H.

Table 1: **Benchmark performance averaged across all videos.** Metrics are normalized to  $[0, 1]$  and higher is better. Best, second-, and third-best values per metric are indicated by bold, underline, and dashed underline, respectively. A video is counted as successful only if every per-video metric passes its calibrated threshold. The uniformly low success rates indicate that meeting all quality criteria simultaneously remains challenging for current open-source video models.

Mode	Model	Bg Stab.	Motion Sim.	App. Stab.	3D Shape Stab.	Physical Plaus.	Success Rate
V2V	Cosmos2.5-2B	<b>0.77</b>	<b>0.60</b>	<u>0.49</u>	<u>0.63</u>	<u>0.71</u>	<b>0.22</b>
	Cosmos2.5-14B	0.55	0.52	<u>0.46</u>	<u>0.59</u>	0.68	0.14
	MAGI-1-4.5B	0.21	<u>0.38</u>	<u>0.38</u>	<u>0.50</u>	<u>0.52</u>	<u>0.01</u>
I2V	Cosmos2.5-2B	0.61	0.51	0.44	0.57	0.66	0.12
	Cosmos2.5-14B	<u>0.51</u>	0.47	0.44	0.56	0.67	0.08
	MAGI-1-4.5B	0.19	0.40	<u>0.46</u>	0.52	0.54	0.02
	CogVideoX1.5-5B	0.39	0.29	<u>0.33</u>	0.40	0.58	0.02
	Wan2.2-14B	<u>0.76</u>	<u>0.59</u>	<b>0.52</b>	<b>0.72</b>	<b>0.73</b>	<u>0.20</u>

**Finding #1:** All evaluated open-source video models fail to reliably generate short clips of basic rigid-body physics. Even the strongest evaluated model achieves only 22% success rate, with most models below 15%.

**Counterfactual consistency.** Figure 5 reports each model’s sensitivity to targeted interventions. All models show substantial variation across interventions. The pattern across intervention types is informative. Appearance changes — which alter only object color while preserving geometry, scene layout, and dynamics — are tolerated best, yet even the most robust models vary by around 20% under this superficial perturbation. Scene and object-category interventions induce larger variation, which is partly expected: changing the object also changes its mass and changing the scene alters geometry that affects the rollout. Viewpoint changes, however, induce the largest variation across most models, despite preserving the underlying 3D dynamics, all object properties, and the scene itself. A model with stable 3D-aware predictions should produce similar physical rollouts across viewpoints.

However, the high observed sensitivity indicates that current models instead encode predictions in a strongly view-dependent way, relying on visual statistics that do not transfer across viewpoints of the same physical event.

**Finding #2:** Models do not achieve robust counterfactual physical consistency: generation quality substantially changes across interventions, with especially high sensitivity to viewpoint and object-category changes.

**Effect of video conditioning.** By comparing I2V and V2V results for Cosmos and MAGI-1 in Table 1 we observe that videos generated in the V2V setting outperform their I2V counterparts in most metrics. This is expected for motion similarity, as additional frames contain information about motion direction and magnitude. Surprisingly, results suggest that video conditioning also decreases the presence of background perturbations for MAGI-1 and the Cosmos family, and it improves object stability in both appearance and shape for the Cosmos family. We hypothesize that video conditioning helps the model to develop more robust object representations at inference time. The improved background stability in the V2V setting could also be explained by the fact that absent camera motion on the conditioning clip might support a more stable camera in the generated video, providing a stronger signal than solely text conditioning as in the I2V setting.

**Finding #3:** Video conditioning generally improves not only motion fidelity, as expected from the additional temporal signal, but also the stability of backgrounds and objects, suggesting that additional conditioning frames can support more stable outputs at inference time.

**Effect of model size.** Comparing Cosmos2.5-2B and Cosmos2.5-14B provides a within-family scale comparison. Surprisingly, the 14B variant performs worse than the 2B variant across nearly

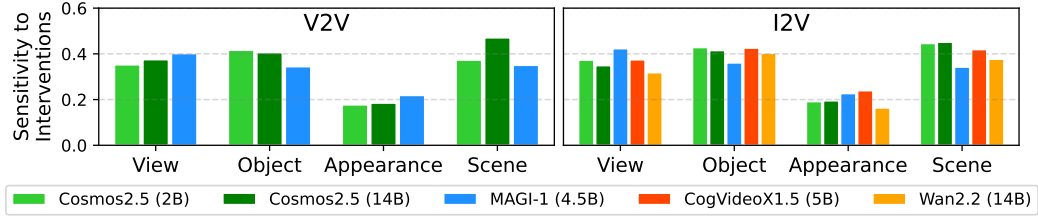


Figure 5: **Sensitivity to counterfactual interventions.** Sensitivities are averaged across metrics, and lower values indicate lower sensitivity. All evaluated models show substantial variation across intervention types, including appearance changes that alter only objects’ visual properties.

every metric in both I2V and V2V settings (Table 1) — including a drop in success rate from 22% to 14% in V2V. This result is consistent with the scaling study of Kang et al. [27] who show in a simplified 2D setting that larger video generators can improve in-distribution prediction without learning physical laws that generalize robustly to out-of-distribution settings. Our finding provides further evidence for this concern on a photorealistic benchmark and modern pretrained open models. As our benchmark measures counterfactual physical consistency, it systematically studies the stability under controlled interventions where physical laws should be satisfied. We note that the observation presented here is based on a single model family and a single scale step, but nevertheless motivates future detailed investigation, which our benchmark enables.

**Finding #4:** Scaling Cosmos from 2B to 14B parameters yields no improvement on physical event generation, indicating that model size alone does not guarantee better counterfactual physical consistency.

## 5 Limitations

**Synthetic-to-real domain gap.** CRONOS uses Unreal Engine renderings rather than real videos. This control is necessary for matched counterfactual interventions and is common in synthetic physics benchmarks [51, 10, 7], but it introduces a domain gap despite the high visual fidelity of the selected scenes. Our results should therefore be read as diagnostic evidence about controlled physical prediction, not as direct estimates of real-video performance.

**Single-reference rollouts.** Most metrics compare a generation to one rendered reference rollout, although the conditioning signal, especially a single I2V frame, permits multiple plausible futures. We account for this with multi-seed evaluation, detailed text prompts, and stability metrics that are independent of the reference. Future versions could evaluate against distributions or sets of physically admissible rollouts.

**Scope of evaluated models.** We evaluate open-source models with fixed weights and reproducible settings, not closed commercial systems such as Veo, Sora, or Kling. This limits coverage of the current model landscape, but the benchmark remains far from saturated: even the strongest evaluated model reaches only 22% success rate.

## 6 Conclusions

We introduce CRONOS, an intervention-based benchmark for evaluating counterfactual physical consistency in video generation models. CRONOS consists of high-quality synthetic videos of controlled physical events, including collisions, falling dynamics, and occlusions. For each event, we systematically intervene on four visual factors—camera viewpoint, object class, background scene, and object appearance—enabling fine-grained analysis of model sensitivity to structured changes. To evaluate predictions, we combine state-of-the-art foundation models, handcrafted rules and VLM-as-a-judge to design a collection of metrics focusing on object stability and physical plausibility that are validated through a user study. Using these metrics under controlled interventions reveals substantial limitations of current video models: even the strongest current video models struggle to generate simple physical events and show substantial variation under targeted visual interventions,

revealing low counterfactual physical consistency. Our findings suggest that many models rely on superficial visual correlations rather than producing stable predictions of scene dynamics. In general, CRONOS provides a useful testbed for diagnosing these limitations and guiding the development of video models that produce more robust and structured predictions of the visual world.

## Acknowledgments and Disclosure of Funding

AK acknowledges support via his Emmy Noether Research Group funded by the German Research Foundation (DFG) under grant number 468670075. This research was funded by the Deutsche Forschungsgemeinschaft (DFG, German Research Foundation) under grant number 539134284, through EFRE (FEIH\_2698644) and the state of Baden-Württemberg.



Baden-Württemberg



Co-funded by  
the European Union

## References

- [1] A. Ali, J. Bai, M. Bala, Y. Balaji, A. Blakeman, T. Cai, J. Cao, T. Cao, E. Cha, Y.-W. Chao, et al. World simulation with video foundation models for physical ai. *arXiv preprint arXiv:2511.00062*, 2025.
- [2] M. Assran et al. Self-supervised learning from video with joint embedding predictive architectures. *arXiv preprint arXiv:2301.08243*, 2023.
- [3] T. Ates, M. S. Atesoglu, C. Yigit, I. Kesen, M. Kobas, E. Erdem, A. Erdem, T. Goksun, and D. Yuret. Craft: A benchmark for causal reasoning about forces and interactions, 2022. URL <https://arxiv.org/abs/2012.04293>.
- [4] S. Bai, Y. Cai, R. Chen, K. Chen, X. Chen, Z. Cheng, L. Deng, W. Ding, C. Gao, C. Ge, et al. Qwen3-vl technical report. *arXiv preprint arXiv:2511.21631*, 2025.
- [5] H. Bansal, Z. Lin, T. Xie, Z. Zong, M. Yarom, Y. Bitton, C. Jiang, Y. Sun, K.-W. Chang, and A. Grover. Videophy: Evaluating physical commonsense for video generation. *arXiv preprint arXiv:2406.03520*, 2024.
- [6] H. Bansal, C. Peng, Y. Bitton, R. Goldenberg, A. Grover, and K.-W. Chang. Videophy-2: A challenging action-centric physical commonsense evaluation in video generation. *arXiv preprint arXiv:2503.06800*, 2025.
- [7] D. M. Bear, E. Wang, D. Mrowca, F. J. Binder, H.-Y. F. Tung, R. Pramod, C. Holdaway, S. Tao, K. Smith, F.-Y. Sun, et al. Physion: Evaluating physical prediction from vision in humans and machines. *arXiv preprint arXiv:2106.08261*, 2021.
- [8] A. Blattmann, T. Dockhorn, S. Kulal, D. Mendeleevitch, M. Kilian, D. Lorenz, Y. Levi, Z. English, V. Voleti, A. Letts, V. Jampani, and R. Rombach. Stable video diffusion: Scaling latent video diffusion models to large datasets. *arXiv preprint arXiv:2311.15127*, 2023.
- [9] A. Blattmann, R. Rombach, H. Ling, T. Dockhorn, S. W. Kim, S. Fidler, and K. Kreis. Align your latents: High-resolution video synthesis with latent diffusion models. In *Proceedings of the IEEE/CVF Conference on Computer Vision and Pattern Recognition (CVPR)*, 2023.
- [10] F. Bordes, Q. Garrido, J. T. Kao, A. Williams, M. Rabbat, and E. Dupoux. Intphys 2: Benchmarking intuitive physics understanding in complex synthetic environments. *arXiv preprint arXiv:2506.09849*, 2025.
- [11] X. Chen, F.-J. Chu, P. Gleize, K. J. Liang, A. Sax, H. Tang, W. Wang, M. Guo, T. Hardin, X. Li, et al. Sam 3d: 3dfy anything in images. *arXiv preprint arXiv:2511.16624*, 2025.
- [12] Y. Chen, X. Zhu, and T. Li. A physical coherence benchmark for evaluating video generation models via optical flow-guided frame prediction, 2025. URL <https://arxiv.org/abs/2502.05503>.

- [13] O. Dünkel, A. Jesslen, J. Xie, C. Theobalt, C. Rupprecht, and A. Kortylewski. CNS-Bench: Benchmarking image classifier robustness under continuous nuisance shifts. In *Proceedings of the IEEE/CVF International Conference on Computer Vision (ICCV)*, pages 19978–19988, 2025.
- [14] Epic Games. *Unreal Engine*, 2025. URL <https://unrealengine.com>. Software.
- [15] W. Feng, J. Li, M. Saxon, T.-j. Fu, W. Chen, and W. Y. Wang. Tc-bench: Benchmarking temporal compositionality in text-to-video and image-to-video generation. *arXiv preprint arXiv:2406.08656*, 2024.
- [16] A. Foss, C. Evans, S. Mitts, K. Sinha, A. Rizvi, and J. T. Kao. CausalVQA: A physically grounded causal reasoning benchmark for video models, 2025. URL <https://arxiv.org/abs/2506.09943>.
- [17] J. Gu, X. Liu, Y. Zeng, A. Nagarajan, F. Zhu, D. Hong, Y. Fan, Q. Yan, K. Zhou, M.-Y. Liu, and X. E. Wang. PhyWorldBench: A comprehensive evaluation of physical realism in text-to-video models, 2025. URL <https://arxiv.org/abs/2507.13428>.
- [18] X. Guo, J. Huo, Z. Shi, Z. Song, J. Zhang, and J. Zhao. T2VPhysBench: A first-principles benchmark for physical consistency in text-to-video generation, 2025. URL <https://arxiv.org/abs/2505.00337>.
- [19] D. Ha and J. Schmidhuber. World models. *arXiv preprint arXiv:1803.10122*, 2018.
- [20] D. Hendrycks and T. G. Dietterich. Benchmarking neural network robustness to common corruptions and perturbations. In *7th International Conference on Learning Representations, ICLR 2019*. OpenReview.net, 2019. URL <https://openreview.net/forum?id=HJz6tiCqYm>.
- [21] J. Ho, W. Chan, C. Saharia, M. Norouzi, and D. Fleet. Imagen video: High definition video generation with diffusion models. *arXiv preprint arXiv:2210.02303*, 2022.
- [22] J. Ho, T. Salimans, A. Gritsenko, W. Chan, M. Norouzi, and D. J. Fleet. Video diffusion models. In *International Conference on Learning Representations (ICLR)*, 2022.
- [23] L. Hu, A. Shankarampeta, Y. Huang, Z. Dai, H. Yu, Y. Zhao, H. Kang, D. Zhao, T. Rosing, and H. Zhang. Benchmarking scientific understanding and reasoning for video generation using VideoScience-Bench, 2025. URL <https://arxiv.org/abs/2512.02942>.
- [24] Z. Huang, F. Zhang, X. Xu, Y. He, J. Yu, Z. Dong, Q. Ma, N. Chanpaisit, C. Si, Y. Jiang, et al. Vbench++: Comprehensive and versatile benchmark suite for video generative models. *IEEE Transactions on Pattern Analysis and Machine Intelligence*, 2025.
- [25] Z. Huang et al. Vbench: Comprehensive benchmark suite for video generative models. *arXiv preprint arXiv:2311.17982*, 2023.
- [26] S. Jassim, M. Holubar, A. Richter, C. Wolff, X. Ohmer, and E. Bruni. Grasp: a novel benchmark for evaluating language grounding and situated physics understanding in multimodal language models. In *Proceedings of the Thirty-Third International Joint Conference on Artificial Intelligence*, pages 6297–6305, 2024.
- [27] B. Kang, Y. Yue, R. Lu, Z. Lin, Y. Zhao, K. Wang, G. Huang, and J. Feng. How far is video generation from world model: A physical law perspective. *arXiv preprint arXiv:2411.02385*, 2024.
- [28] N. Karaev, Y. Makarov, J. Wang, N. Neverova, A. Vedaldi, and C. Rupprecht. Cotracker3: Simpler and better point tracking by pseudo-labelling real videos. In *Proceedings of the IEEE/CVF International Conference on Computer Vision*, pages 6013–6022, 2025.
- [29] W. Kong, Q. Tian, Z. Zhang, R. Min, Z. Dai, J. Yao, G. Zhu, T. Fang, H. Wu, Y. Ai, et al. Hunyuanvideo: A systematic framework for large video generative models. *arXiv preprint arXiv:2412.03603*, 2024.

- [30] C. Li, O. Michel, X. Pan, S. Liu, M. Roberts, and S. Xie. Pisa experiments: Exploring physics post-training for video diffusion models by watching stuff drop. In *International Conference on Machine Learning*, pages 35685–35709. PMLR, 2025.
- [31] D. Li, Y. Fang, Y. Chen, S. Yang, S. Cao, J. Wong, M. Luo, X. Wang, H. Yin, J. E. Gonzalez, et al. Worldmodelbench: Judging video generation models as world models. *arXiv preprint arXiv:2502.20694*, 2025.
- [32] Y. Liu, X. Cun, X. Liu, X. Wang, Y. Zhang, H. Chen, Y. Liu, T. Zeng, R. Chan, and Y. Shan. Evalcrafter: Benchmarking and evaluating large video generation models. In *Proceedings of the IEEE/CVF conference on computer vision and pattern recognition*, pages 22139–22149, 2024.
- [33] X. Ma, Y. Wang, G. Jia, X. Chen, Z. Liu, Y.-F. Li, C. Chen, and Y. Qiao. Latte: Latent diffusion transformer for video generation. *arXiv preprint arXiv:2401.03048*, 2024.
- [34] Z. Ma, M. Liufu, and G. Gkioxari. Out of sight, out of mind? evaluating state evolution in video world models. *arXiv preprint arXiv:2603.13215*, 2026.
- [35] F. Meng, J. Liao, X. Tan, W. Shao, Q. Lu, K. Zhang, Y. Cheng, D. Li, Y. Qiao, and P. Luo. Towards world simulator: Crafting physical commonsense-based benchmark for video generation. *arXiv preprint arXiv:2410.05363*, 2024.
- [36] S. Motamed, L. Culp, K. Swersky, P. Jaini, and R. Geirhos. Do generative video models understand physical principles?, 2025. URL <https://arxiv.org/abs/2501.09038>.
- [37] M. Oquab, T. Darcet, T. Moutakanni, H. Vo, M. Szafraniec, V. Khalidov, P. Fernandez, D. Haziza, F. Massa, A. El-Nouby, et al. Dinov2: Learning robust visual features without supervision. *arXiv preprint arXiv:2304.07193*, 2023.
- [38] J. Pearl. *Causality: Models, Reasoning and Inference*. Cambridge University Press, 2009.
- [39] A. Polyak, A. Zohar, A. Brown, A. Tjandra, A. Sinha, A. Lee, A. Vyas, B. Shi, C.-Y. Ma, C.-Y. Chuang, et al. Movie gen: A cast of media foundation models. *arXiv preprint arXiv:2410.13720*, 2024.
- [40] T. Ressler-Antal, F. Fundel, M. B. Alaya, S. A. Baumann, F. Krause, M. Gui, and B. Ommer. Dismo: Disentangled motion representations for open-world motion transfer. In *The Thirty-ninth Annual Conference on Neural Information Processing Systems*, 2025.
- [41] J. Richens and T. Everitt. Robust agents learn causal world models. In *The Twelfth International Conference on Learning Representations*, 2024.
- [42] B. Schölkopf, F. Locatello, S. Bauer, N. R. Ke, N. Kalchbrenner, A. Goyal, and Y. Bengio. Toward causal representation learning. *Proceedings of the IEEE*, 109(5):612–634, 2021.
- [43] M. Shu, C. Liu, W. Qiu, and A. L. Yuille. Identifying model weakness with adversarial examiner. In *Proceedings of the AAAI Conference on Artificial Intelligence*, pages 11998–12006. AAAI Press, 2020. doi: 10.1609/aaai.v34i07.6876.
- [44] U. Singer, A. Polyak, T. Hayes, X. Yin, J. An, S. Zhang, Q. Hu, H. Yang, O. Ashual, O. Gafni, D. Parikh, S. Gupta, and Y. Taigman. Make-a-video: Text-to-video generation without text-video data. *arXiv preprint arXiv:2209.14792*, 2022.
- [45] H. Teng, H. Jia, L. Sun, L. Li, M. Li, M. Tang, S. Han, T. Zhang, W. Zhang, W. Luo, et al. Magi-1: Autoregressive video generation at scale. *arXiv preprint arXiv:2505.13211*, 2025.
- [46] H.-Y. Tung, M. Ding, Z. Chen, D. Bear, C. Gan, J. Tenenbaum, D. Yamins, J. Fan, and K. Smith. Physion++: Evaluating physical scene understanding that requires online inference of different physical properties. *Advances in Neural Information Processing Systems*, 36:67048–67068, 2023.
- [47] T. Unterthiner, S. Van Steenkiste, K. Kurach, R. Marinier, M. Michalski, and S. Gelly. Towards accurate generative models of video: A new metric & challenges. *arXiv preprint arXiv:1812.01717*, 2018.

- [48] R. Upadhyay, H. Zhang, J. Solomon, A. Agrawal, P. Boreddy, S. S. Narayana, Y. Ba, A. Wong, C. M. de Melo, and A. Kadambi. Worldbench: Disambiguating physics for diagnostic evaluation of world models. *arXiv preprint arXiv:2601.21282*, 2026.
- [49] T. Wan, A. Wang, B. Ai, B. Wen, C. Mao, C.-W. Xie, D. Chen, F. Yu, H. Zhao, J. Yang, et al. Wan: Open and advanced large-scale video generative models. *arXiv preprint arXiv:2503.20314*, 2025.
- [50] Z. Yang, J. Teng, W. Zheng, M. Ding, S. Huang, J. Xu, Y. Yang, W. Hong, X. Zhang, G. Feng, et al. Cogvideox: Text-to-video diffusion models with an expert transformer. *arXiv preprint arXiv:2408.06072*, 2024.
- [51] K. Yi, C. Gan, Y. Li, P. Kohli, J. Wu, A. Torralba, and J. B. Tenenbaum. Clevrer: Collision events for video representation and reasoning. In *International Conference on Learning Representations*, 2020.
- [52] C. Zhang, D. Cherniavskii, A. Tragoudaras, A. Vozikis, T. Nijdam, D. W. E. Prinzhorn, M. Bodracska, N. Sebe, A. Zadaianchuk, and E. Gavves. Morpheus: Benchmarking physical reasoning of video generative models with real physical experiments, 2025. URL <https://arxiv.org/abs/2504.02918>.
- [53] Q. Zhang, P. Jing, H.-X. Yu, F. Ding, F. Nie, W. Wang, Y. Du, J. Zou, J. Wu, and B. Shuai. Physion-eval: Evaluating physical realism in generated video via human reasoning, 2026. URL <https://arxiv.org/abs/2603.19607>.
- [54] D. Zheng, Z. Huang, H. Liu, K. Zou, Y. He, F. Zhang, L. Gu, Y. Zhang, J. He, W.-S. Zheng, et al. Vbench-2.0: Advancing video generation benchmark suite for intrinsic faithfulness. *arXiv preprint arXiv:2503.21755*, 2025.

## A Dataset details

The dataset of CRONOS is handcrafted using combinations of object and scene assets. Objects are selected to align with the physical events under study, ensuring that their geometry and material properties allow sliding or rolling over smooth surfaces, thereby producing visually plausible and dynamically rich motion patterns. Simulated physical parameters, including mass, friction, and restitution coefficients, are explicitly defined per object and are kept consistent across events. Scene layouts and initial conditions (e.g., object positions and applied forces), are individually tailored to fit each physical event, and camera viewpoints are strategically positioned to preserve global context while maintaining clear visibility of the relevant interactions throughout the sequence. This ensures that differences between rendered videos are attributable only to controlled interventions on the scene state. The proposed controlled generation process forms the basis for the construction of matched counterfactual observations used throughout CRONOS. Table 2 shows the number of different variations per intervention type. An overview of the original asset scenes, objects used for interventions and their different appearances are shown in Figure 6.

For all three physical events, all variations are rendered. The only exception is the occlusion event, where the view is not altered to preserve the intended visibility effect. The number of videos rendered per event is shown in Table 3.

Table 2: **Number of variations per intervention.** Table 3: **Number of videos per physical event.**

Intervention	# of variations
Scene	5
Object	5
View	4
Appearance	3

Event	# of videos
Fall	300
Collision	300
Occlusion	75
Total	675

## B Text Prompts

In addition to the visual conditioning signal, text prompts are provided to all video models. These prompts have been manually designed for each physical event, and follow the same structure across interventions, as shown in 4. The prompts coarsely describe each physical event, serving as an overview of the expected dynamics but without providing many details. The specific variation values of each intervention type are added through the prompt, as well as details required by each physical event (e.g., the collision target and the occluding object). On top of this, an additional shared prompt is added in all cases, providing general details about the expected physical behavior and camera movement.

## C Evaluation details

**Robust minimum and maximum estimation.** Observing generated videos, we realized that alterations or hallucinations in a few frames can completely change the way humans perceive the video. Therefore, aggregating per-frame results using the average is not convenient, as the effect of a brief but meaningful error gets diminished. On the other hand, considering only the worst frame is unstable and can be affected by limitations of our metrics. Instead, we compute the average of the worst  $k$  frames in the video. We select  $k$  to be around 5% of the total generated frames. In cases where we compute scores per object, we select the worst  $k$  scores across both sets of values. This way, videos where a single object behaves unrealistically do not get their scores averaged by the other object.

**Object segmentation masks and point tracks.** For all videos, we estimate per-object segmentation masks using SAM3 and point tracks using CoTracker3 Karaev et al. [28]. In both cases, we prompt the model with the original rendered masks in the first frame, which always matches the ground truth renders. We then propagate through the video to obtain per-frame predictions.



Figure 6: **Dataset assets.** Overview of Unreal Engine assets used for all rendered sequences: original scenes, object models, and appearance variations.

**Object disappearance detection.** Videos in which objects vanish abruptly can yield artificially inflated scores on object-centric metrics, since evaluation is only meaningful on frames where the target object is present. At the same time, given our video settings, we must account for legitimate effects such as occlusion and objects leaving the scene. To disentangle these cases, we introduce an object disappearance detector. A disappearance is registered only when two criteria are jointly satisfied: (i) the object is absent from the disappearance frame onward, and (ii) the object does not exit the image boundary at the disappearance time. We assess the first criterion using the predicted segmentation masks and the second using object tracks, which extrapolate motion beyond the visible frame. Because very rapidly vanishing objects might artificially obtain high scores in some metrics, we conservatively assign videos containing disappearing objects the minimum score on appearance stability, shape stability, and motion similarity.

**Occlusion filter.** Beyond disappearance detection, object-level metrics (appearance and shape stability) operate on segmentation masks and therefore require a sufficient number of visible pixels to be reliable. Under severe occlusion, these metrics become unstable. To mitigate this, we introduce an occlusion filter that restricts metric computation to frames with low occlusion. We estimate the occlusion level of an object as the ratio between its current mask size and its mask size in the first frame. We find this simple heuristic to be effective in practice, as the apparent size of objects remains approximately constant across most videos in our setting. For each object, we retain only frames in which the estimated visible fraction exceeds a threshold of 25% of the initial mask size, and we apply this selection independently per object.

Table 4: **Structure of text prompts.** General text prompt structure for each physical event. Variables in brackets are substituted using the details of each particular video. An additional prompt describing the general physical behavior and expected movement is added to all physical events.

Event	Prompt Structure
Fall	The video shows a {view} view of a {appearance}{object} smoothly {object_movement} across a {surface} in a {scene}. When the {object} reaches the edge, it falls off the {surface} and vertically descends until it hits the ground. The object maintains its shape and does not break during the fall.
Collision	The video shows a {view} view of a {appearance}{object} smoothly {object_movement} across a {surface}, colliding with a {collision_target} in a {scene}. The objects react to the collision but preserve their rigidity and do not break.
Occlusion	The video shows a {view} view of a {appearance}{object} smoothly {object_movement} and passing behind a {occluding_object} on a {surface} in a {scene}. The {object} becomes temporarily occluded by the {occluding_object} before reappearing. The {occluding_object} remains stationary throughout the sequence.
Additional prompt	Everything in the video follows the natural behavior of solid objects in a physical environment. Objects do not fly, morph, or disappear. No new elements appear in the scene. The background is static. Fixed camera view, no camera movement.

**Object stability.** This metric quantifies semantic distortions of objects across the generated videos. For that, we compare all generated frames with the first context frame, which matches the original render. For a given frame  $I^t$ , we mask each object ( $I_i^t$ ) and extract its CLS token using DINOv2. Then, we compute the cosine similarity between the tokens from the first and subsequent frames. The stability metric is computed by taking our robust minimum across the video and across objects. This way, the metric is sensitive to object alterations which happen only in a few frames or only happen to a single object. We compute

$$\text{ObjectStability} = \text{RobustMin}_{i,t} (\langle \text{CLS}(I_i^t) \cdot \text{CLS}(I_i^0) \rangle), \quad (1)$$

where  $\langle \cdot \rangle$  denotes the cosine similarity.

**Background stability** Complementary to the object stability metric, we quantify alterations on the background, which should remain static in all sequences. This way, we are able to detect morphing, new objects appearing, and camera movement. We measure changes by comparing all generated frames to the initial reference frame via pixel-wise MSE:

$$\text{BackgroundStability} = \text{RobustMax}_t (\text{MSE}(\text{BG}(I^t), \text{BG}(I^0))). \quad (2)$$

For every frame, only background pixels shared between both images are considered. The shared background is computed as the intersection between the background mask of both frames. In this case, we use robust maximum operation to focus on frames where the background is heavily altered. In order to scale this metric into the  $[0, 1]$  range, we apply decaying exponential scaling  $S' = \exp[-50 \cdot S]$ .

**Motion similarity.** The introduced metric to evaluate motion is based on the motion encoder from DisMo. This model encodes abstract representations that are independent from appearance or object

identity. This way, we are able to disentangle motion from visual properties, without relying on simplistic metrics, such as comparing object centroid position. The metric is computed by taking the robust minimum over the video of the cosine similarity of the embeddings from the reference and generated video,

$$\text{MotionSimilarity} = \text{RobustMin}_t \left( \langle \text{DisMo}(I^t) \cdot \text{DisMo}(\tilde{I}^t) \rangle \right), \quad (3)$$

where  $\tilde{I}$  indicates the reference frames.

**Shape stability.** Object shape is usually overlooked or indirectly measured in other benchmarks. We take advantage of advances in 3D shape estimation models to design a novel metric to quantify object morphing in video models. We run SAM3D on the generated videos by prompting the model with the object segmentation masks predicted by SAM3, and obtain object meshes  $M_i^t$ . For each video, we align all meshes to the reference by optimizing scale and rotation. For each object  $i$ , we compute the Chamfer Distance (CD) between predicted meshes for the initial and all subsequent frames,

$$\text{ShapeStability} = \text{RobustMax}_{i,t} \left( \text{CD}(M_i^t, M_i^0) \right). \quad (4)$$

We again apply the exponential scaling used for background stability to bring CD into the  $[0, 1]$  range.

**Physical plausibility.** This metric is used to capture high level information about the physical events in the video, as well as detecting events which are hard to automatically generalize for arbitrary videos. We design 5 general questions, as well as 5 templates for each physical event. The templates are individually adjusted for each video by substituting sequence-specific details, such as object classes. The prompt is:

**VLM judge input prompt**

You are evaluating a short video of a physics simulation. An object in the scene was pushed just before the video starts. Watch the video carefully and answer all of the following questions about what you observe. For each question provide a True or False answer. Provide brief comments justifying your answers and rate your overall confidence from 0.0 (not confident at all) to 1.0 (fully confident).

Video description: <video\_description>

Questions: <video\_questions>

"Respond ONLY with valid JSON using exactly this structure (no extra text outside the JSON):",

```
{
  "answers": {
    "question_key1": <answer1>,
    ...
  },
  "comments": "<brief justification for each answer>",
  "confidence": <float 0.0–1.0>
}
```

And the specific questions can be found in Table 5. The final metric is computed by collecting the fraction of questions that do not match the expected outcome and applying inverse scaling:

$$\text{PhysicalPlausibility} = \left( 1 + \sum_b \mathbf{1}[b_{\text{VLM}} \neq b_{\text{Ideal}}] \right)^{-1}. \quad (5)$$

This way, a video collecting a few negative answers will result in low physical plausibility, compared to a linear metric, where the video would still receive a high score.

Table 5: **Questions for physical plausibility metric.**

Event	Questions
Fall	Does the {object_name} fall off the {surface} when it reaches the edge? Does the {object_name} hit the ground? Does the {object_name} change its direction while falling? Does the {object_name} move on an arc-shaped path while falling? Does the {object_name} accelerate while falling?
Collision	Does the {object_name} contact with the {collision_target}? Does the {object_name} come to a stop before contacting the {collision_target}? Is the motion of {object_name} affected by the collision with the {collision_target}? Is the reaction to the impact realistic considering the size and mass of the objects? Are objects deformed or broken during or after the collision?
Occlusion	Does the {object_name} move behind the {occluding_object} during the video? Does the {object_name} reappear on the other side after being occluded by the {occluding_object}? Does the {object_name} move on a straight path during the whole video? Does the {object_name} disappear after being occluded by the {occluding_object}? Does the {object_name} change its appearance after being occluded by the {occluding_object}?
Shared questions	Is the background static throughout the video? Does the {object_name} maintain its color and shape throughout the video? Do new objects appear on the scene during the video? Do objects move smoothly without sudden jumps or teleportation during the video? Do objects move without forces acting on them?

**Success rate.** We compress the quality of each video by calibrating thresholds in all our metrics. This way, we prevent catastrophic failures in one metric from being smoothed by other results. The thresholds are calibrated using the human study. We consider successful videos in an annotated metric as those which achieve a median score of 3 or higher. We then calibrate thresholds on the corresponding metrics by minimizing the absolute difference between false positive rate and false negative rate. The specific thresholds for every metric are shown in 6.

Table 6: **Metric thresholds for success rate.** Only videos exceeding the calibrated thresholds are labeled as successful.

Metric	Threshold
Appearance stability	0.48
Background stability	0.30
Motion similarity	0.57
Shape stability	0.60
Physical plausibility	0.48

## D User Study

We present the instructions of the user study in Figure 7 and the GUI for annotating videos along the considered quality axis in Figure 8. All annotators received detailed instructions and needed to pass a

### Evaluation of Generated Videos - Instructions

*These instructions are equivalent to the qualification instructions. Revise them if needed to ensure precise answers are given. We check samples and revoke qualification when answers are not reasonable.*

Welcome to our video model study!

You will help us evaluate AI-generated videos of objects in everyday scenarios. Each video begins with an object (e.g., a bottle, can, tennis ball, soccer ball, or toy truck) that has been pushed. There are three types of videos: fall, collision, and occlusion:

**Fall:** An object rolls along a surface, falls off the edge, and hits the floor.

**Collision:** An object rolls on a flat surface and collides with another stationary object.

**Occlusion:** An object rolls on a flat surface, passes behind another object (becoming temporarily hidden), and then reappears on the other side.

The videos are expected to show realistic physical behavior as objects interact with each other and their environment. For each video, you will evaluate several aspects using a scale from 1 to 5.

Evaluation Dimensions:

**a. Object Appearance**

A high score means the objects maintain consistent color, texture, and identity throughout the video.  
A low score means the objects change color or texture, deform, or merge with other objects.

**b. Object Shape**

A high score means the object's shape remains unchanged.  
A low score indicates visible deformation or distortion of the object.

**c. Background Stability**

A high score means the background remains consistent and the camera is stable.  
A low score means the background changes, new objects appear, or the camera moves unexpectedly.

**d. Motion Plausibility**

A high score means object's motion follows realistic physical behavior, including effects of velocity, mass, gravity, and friction.  
A low score indicates unrealistic motion, such as unexplained changes in direction, floating, or ignoring gravity.

**e. Event Quality**

A high score means the intended physical event (collision, fall, or occlusion) occurs clearly and realistically.  
A low score means the event is missing, unclear, or physically implausible. For example, objects may not respond to a collision, may fail to fall correctly, or may not reappear after being occluded.

For object appearance and shape, only consider the objects visible in the first frame: single object for fall and occlusion, two objects for collision. New objects appearing in the scene should be considered background.

Base your judgments only on what is visible in the video. Do not make assumptions or infer information beyond what is shown.

Figure 7: Instructions of the user study.

qualification exam before participation. The 8 hired Prolific annotators received a compensation of 14 £/hour.

## E Additional examples

In 9, 10 and 11 we show the complete set of generated videos for the examples in 3.

## F Broader impacts

**Potential positive impacts.** CRONOS is an evaluation benchmark for counterfactual physical consistency in video generation models. Its main intended benefit is diagnostic: the benchmark exposes failures such as object drift, broken object permanence, implausible motion, and sensitivity to changes in viewpoint, scene, object category, or appearance. Identifying these failures can help researchers avoid overestimating the physical reliability of visually plausible video predictions.

**Potential negative impacts.** The same diagnostic signal could also guide improvements to video generators that make synthetic videos more physically plausible. Such improvements may increase the realism of misleading or deceptive synthetic media. A second risk is over-interpretation: strong performance on CRONOS would not necessarily imply that a model has learned general physical reasoning or is suitable for safety-critical use. The benchmark covers a limited set of synthetic rigid-body events and should not be treated as a deployment certificate.

**Data, privacy, and release considerations.** The benchmark videos are rendered in a synthetic Unreal Engine environment rather than recorded from real scenes. This reduces privacy risks associated with real-world video datasets. Any release of rendered videos, annotations, generation code, or evaluation code should document the intended use, known limitations, and applicable licenses for rendered assets and third-party tools. In particular, release notes should make clear that

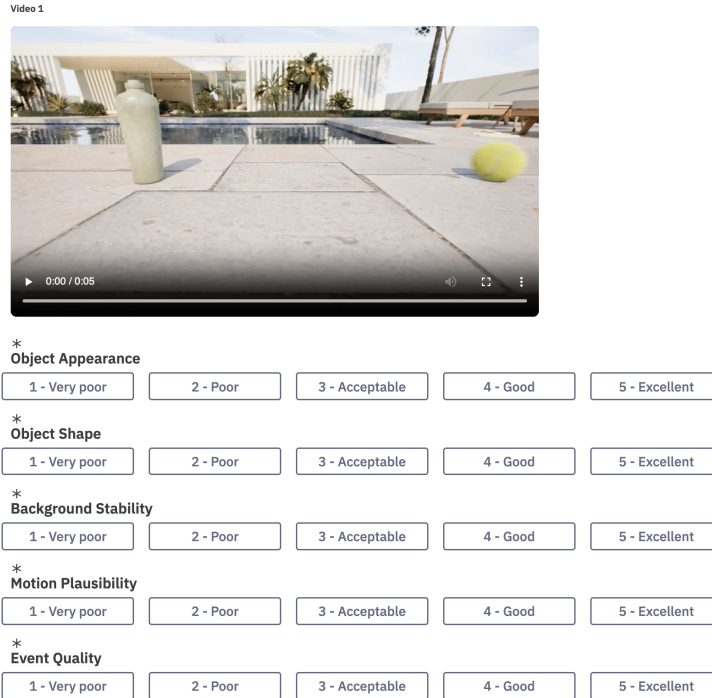


Figure 8: GUI used in the user for annotating video quality.

CRONOS evaluates a narrow set of controlled events and should not be used to claim broad physical competence.

**Environmental considerations.** The benchmark requires rendering high-resolution videos and running several model-based evaluation components, including segmentation, 3D reconstruction, motion encoding, and VLM judging. These steps add computational cost beyond standard video generation evaluation.

## G Asset Licenses and Release Documentation

CRONOS uses third-party Unreal Engine scene assets to construct the rendered simulation environments. All 3D assets were purchased under Epic Content License Agreement (ECLA), and selected only when authors allowed GenAI-related research and benchmark generation. We use the assets as part of controlled synthetic scenes rendered in Unreal Engine; the benchmark does not rely on scraped videos or unlicensed real-world footage.

We release the generated benchmark videos and evaluation code. The release includes the rendered RGB videos, text prompts, benchmark metadata describing the physical event and intervention values for each video, and the code used to compute the evaluation metrics reported in the paper.

We do not redistribute third-party Unreal Engine source assets whose licenses restrict redistribution. Instead, released artifacts are limited to the generated benchmark data, code, and metadata that can be shared under the applicable licenses. The released package will include license information for the dataset and code, along with attribution and license notes for third-party tools and assets used to construct the benchmark.

## H Detailed results

We provide additional results below.



Figure 9: Additional generated examples.

## I Computational resources

We provide an overview of the computational resources in Table 10.



Figure 10: Additional generated examples.

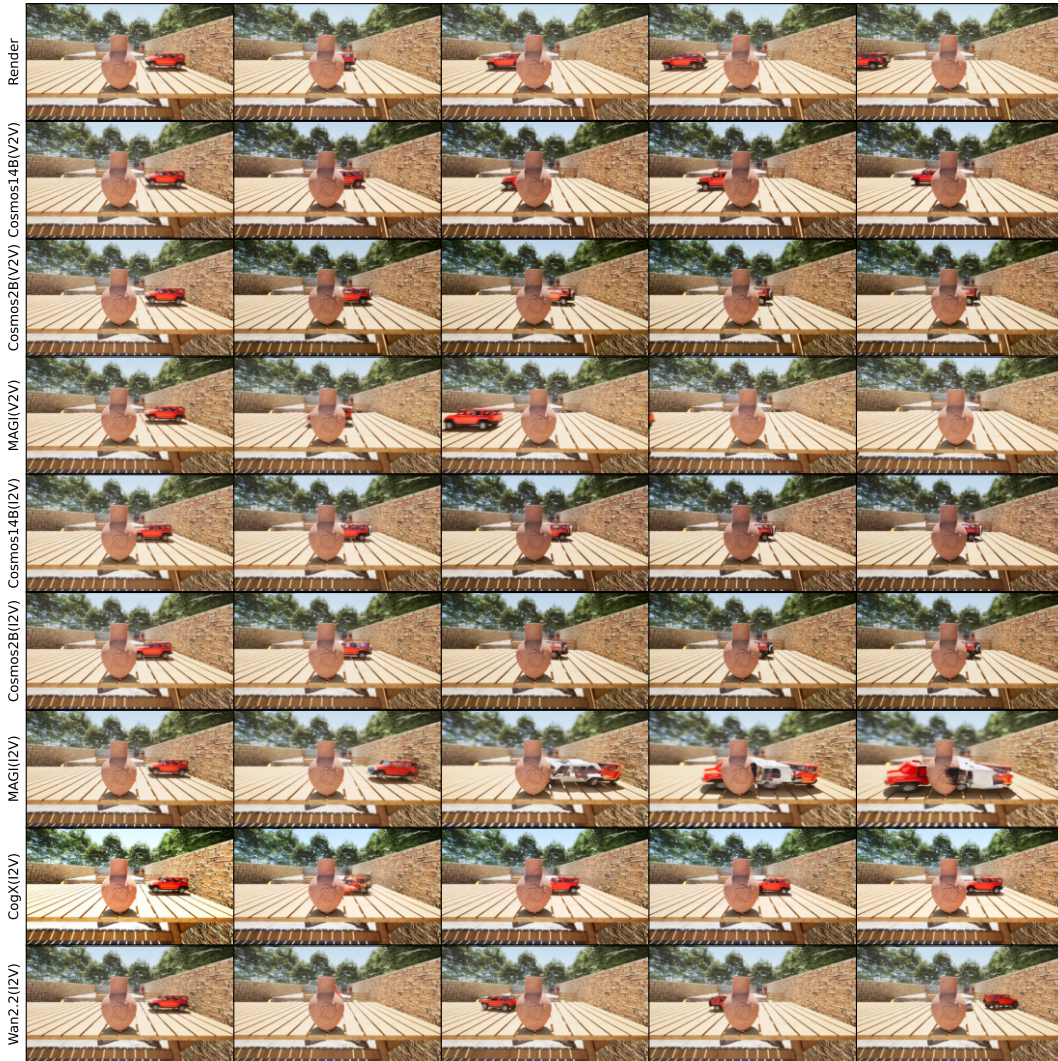


Figure 11: Additional generated examples.

Table 7: Benchmark results per physical event.

Fall							
Mode	Model	Bg Stab.	Motion Sim.	App. Stab.	3D Shape Stab.	Physical Plaus.	Success Rate
V2V	Cosmos2.5-2B	0.80	0.60	0.48	0.57	<b>0.47</b>	0.15
	Cosmos2.5-14B	0.58	0.51	0.43	0.51	0.43	0.10
	MAGI-1-4.5B	0.23	0.40	0.38	0.48	0.39	0.00
I2V	Cosmos2.5-2B	0.64	0.48	0.42	0.51	0.45	0.08
	Cosmos2.5-14B	0.56	0.45	0.41	0.50	0.43	0.06
	MAGI-1-4.5B	0.21	0.40	0.45	0.49	0.40	0.02
	CogVideoX1.5-5B	0.40	0.32	0.36	0.43	0.41	0.01
	Wan2.2-14B	<b>0.83</b>	<b>0.68</b>	<b>0.55</b>	<b>0.72</b>	<b>0.47</b>	<b>0.23</b>
Collision							
Mode	Model	Bg Stab.	Motion Sim.	App. Stab.	3D Shape Stab.	Physical Plaus.	Success Rate
V2V	Cosmos2.5-2B	<b>0.79</b>	<b>0.63</b>	<b>0.52</b>	0.73	0.91	<b>0.30</b>
	Cosmos2.5-14B	0.52	0.54	0.50	0.73	0.86	0.18
	MAGI-1-4.5B	0.22	0.35	0.36	0.52	0.58	0.01
I2V	Cosmos2.5-2B	0.57	0.55	0.48	0.65	0.81	0.16
	Cosmos2.5-14B	0.46	0.50	0.47	0.65	0.84	0.09
	MAGI-1-4.5B	0.22	0.37	0.43	0.53	0.62	0.01
	CogVideoX1.5-5B	0.36	0.23	0.28	0.35	0.65	0.01
	Wan2.2-14B	0.67	0.53	0.49	<b>0.74</b>	<b>0.94</b>	0.17
Occlusion							
Mode	Model	Bg Stab.	Motion Sim.	App. Stab.	3D Shape Stab.	Physical Plaus.	Success Rate
V2V	Cosmos2.5-2B	0.59	0.52	0.43	0.44	0.93	0.19
	Cosmos2.5-14B	0.55	0.47	0.43	0.38	0.88	0.14
	MAGI-1-4.5B	0.11	0.43	0.45	0.48	0.74	0.02
I2V	Cosmos2.5-2B	0.59	0.50	0.41	0.48	0.92	0.15
	Cosmos2.5-14B	0.56	0.48	0.42	0.42	0.89	0.13
	MAGI-1-4.5B	0.10	0.45	<b>0.54</b>	<b>0.58</b>	0.73	0.06
	CogVideoX1.5-5B	0.42	0.42	0.38	0.47	0.93	0.09
	Wan2.2-14B	<b>0.84</b>	<b>0.53</b>	0.52	0.57	<b>0.97</b>	<b>0.21</b>

Table 8: **Benchmark sensitivities per metric.**

Fall						
Mode	Model	Scene	Object	Appearance	View	Average
V2V	Cosmos2.5-2B	0.35	0.37	0.18	0.35	0.31
	Cosmos2.5-14B	0.45	0.37	0.17	0.35	0.34
	MAGI-1-4.5B	0.31	<b>0.31</b>	0.20	0.36	0.30
I2V	Cosmos2.5-2B	0.41	0.40	0.18	0.34	0.33
	Cosmos2.5-14B	0.44	0.41	0.18	0.32	0.34
	MAGI-1-4.5B	<b>0.29</b>	0.34	0.22	0.40	0.31
	CogVideoX1.5-5B	0.36	0.40	0.22	0.34	0.33
	Wan2.2-14B	0.34	0.39	<b>0.14</b>	<b>0.29</b>	<b>0.29</b>
Collision						
Mode	Model	Scene	Object	Appearance	View	Average
V2V	Cosmos2.5-2B	0.37	0.44	<b>0.17</b>	0.35	<b>0.33</b>
	Cosmos2.5-14B	0.48	0.43	0.18	0.40	0.37
	MAGI-1-4.5B	0.37	<b>0.36</b>	0.23	0.44	0.35
I2V	Cosmos2.5-2B	0.48	0.45	0.21	0.41	0.39
	Cosmos2.5-14B	0.45	0.41	0.18	0.37	0.35
	MAGI-1-4.5B	<b>0.35</b>	<b>0.36</b>	0.22	0.44	0.34
	CogVideoX1.5-5B	0.49	0.45	0.27	0.40	0.40
	Wan2.2-14B	0.43	0.41	0.18	<b>0.34</b>	0.34
Occlusion						
Mode	Model	Scene	Object	Appearance		Average
V2V	Cosmos2.5-2B	0.46	0.47	<b>0.20</b>		0.38
	Cosmos2.5-14B	0.51	0.46	0.25		0.41
	MAGI-1-4.5B	0.41	<b>0.39</b>	0.22		0.34
I2V	Cosmos2.5-2B	0.44	0.44	<b>0.20</b>		0.36
	Cosmos2.5-14B	0.48	0.46	0.28		0.41
	MAGI-1-4.5B	0.47	0.42	0.26		0.39
	CogVideoX1.5-5B	0.36	0.45	0.21		0.34
	Wan2.2-14B	<b>0.31</b>	0.44	<b>0.20</b>		<b>0.31</b>

Table 9: **Human study results.** Average median human annotation score per model and metric, 1–5 scale, higher is better.

Mode	Model	Object Appear.	Object Shape	Bg Stab.	Motion Plaus.	Event Quality
V2V	Cosmos2.5-2B	3.65	3.30	<b>4.44</b>	1.62	1.88
	Cosmos2.5-14B	3.70	3.33	3.88	1.76	1.94
	Magi-1-4.5B	2.57	2.57	2.26	1.40	1.33
I2V	Cosmos2.5-2B	3.42	3.29	3.92	1.53	1.68
	Cosmos2.5-14B	3.47	3.14	3.83	1.76	1.91
	Magi-1-4.5B	2.62	2.70	2.20	1.38	1.29
	CogVideoX1.5-5B	1.59	1.37	2.78	1.08	1.16
	Wan2.2-14B	<b>4.15</b>	<b>4.03</b>	4.21	<b>2.33</b>	<b>2.68</b>

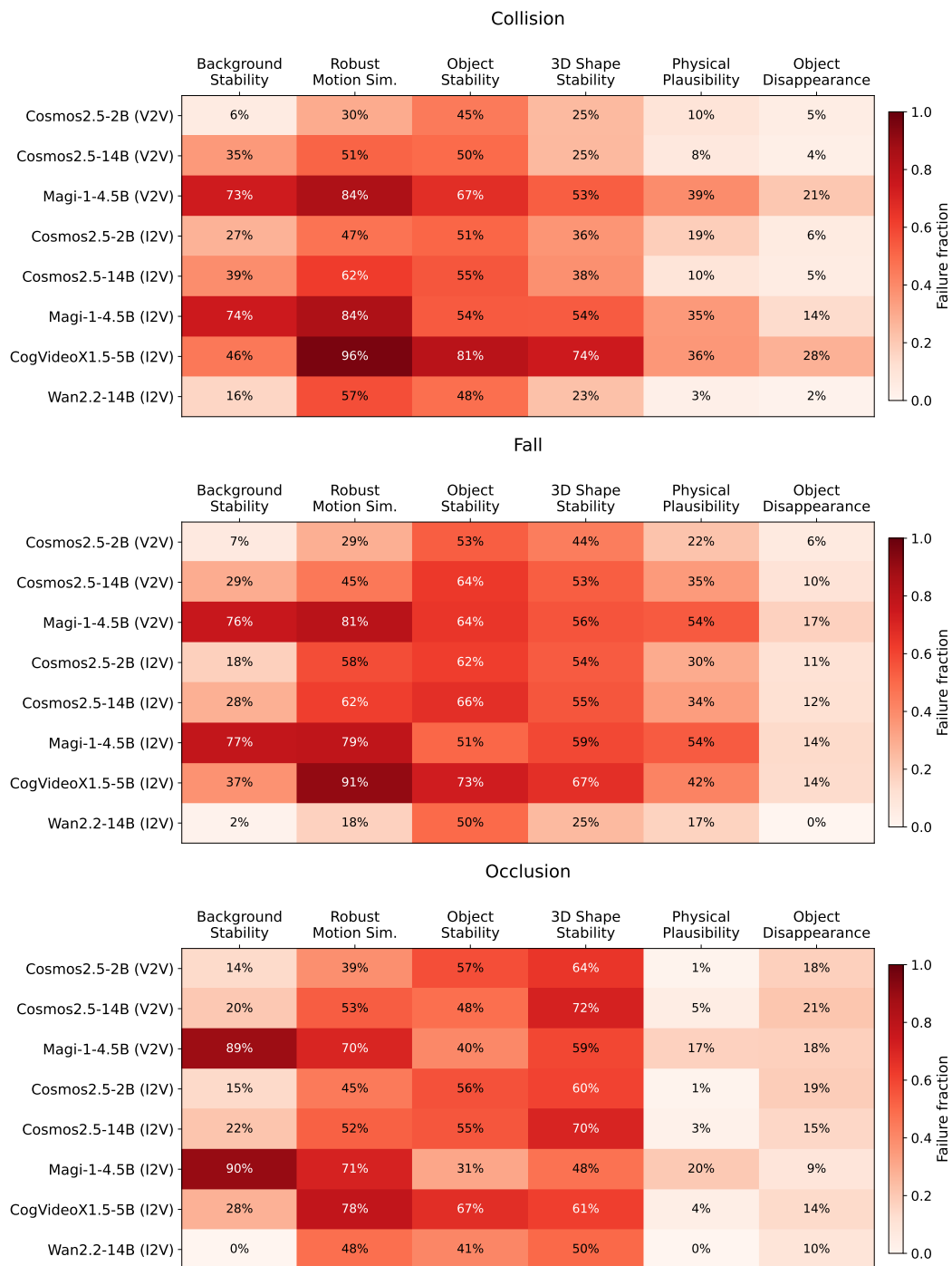


Figure 12: **Failure rates per metric.** For each event, we provide the fraction of videos failing in each metric.

Table 10: **Compute used for benchmark generation and evaluation.** For each evaluated model configuration, 2025 videos were generated. Generation was performed on NVIDIA H100 GPUs, while evaluation was performed on NVIDIA A100 GPUs.

Model	Generation (H100 h)	Evaluation (A100 h)
Cosmos2.5-2B (I2V)	150	60
Cosmos2.5-2B (V2V)	150	60
Cosmos2.5-14B (I2V)	510	60
Cosmos2.5-14B (V2V)	510	60
MAGI-1-4.5B (I2V)	510	60
MAGI-1-4.5B (V2V)	510	60
Wan2.2-14B	840	60
CogVideoX1.5-5B (I2V)	675	60
<b>Total</b>	<b>3855</b>	<b>480</b>